THE JOURNAL OF BIOLOGICAL CHEMISTRY VOL. 282, NO. 23, pp. 17041–17052, June 8, 2007

Disruption of the Aspartate to Heme Ester Linkage in Human Myeloperoxidase

*IMPACT ON LIGAND BINDING, REDOX CHEMISTRY, AND INTERCONVERSION OF REDOX INTERMEDIATES**

Received for publication, November 17, 2006, and in revised form, April 12, 2007 Published, JBC Papers in Press, April 16, 2007, DOI 10.1074/jbc.M610685200

Martina Zederbauer[‡], Paul G. Furtmüller[‡], Marzia Bellei[§], Johanna Stampler[‡], Christa Jakopitsch[‡], Gianantonio Battistuzzi[§], Nicole Moguilevsky[¶], and Christian Obinger[‡1]

From the [‡]Division of Biochemistry, Department of Chemistry, BOKU-University of Natural Resources and Applied Life Sciences, Muthgasse 18, A-1190 Vienna, Austria, the [§]Department of Chemistry, University of Modena and Reggio Emilia, Via Campi 183, I-41100 Modena, Italy, and the [¶]Head of Technology Transfer Office, University of Namur, 53 Rue de Bruxelles, B-5000 Namur, Belgium

In human heme peroxidases the prosthetic group is covalently attached to the protein via two ester linkages between conserved glutamate and aspartate residues and modified methyl groups on pyrrole rings A and C. Here, monomeric recombinant myeloperoxidase (MPO) and the variants D94V and D94N were produced in Chinese hamster ovary cell lines. Disruption of the Asp[94] to heme ester bond decreased the one-electron reduction potential E'_0 [Fe(III)/Fe(II)] from 1 to −55 mV at pH 7.0 and 25 °C, whereas the kinetics of binding of low spin ligands and of compound I formation was unaffected. By contrast, in both variants rates of compound I reduction by chloride and bromide (but not iodide and thiocyanate) were substantially decreased compared with the wild-type protein. Bimolecular rates of compound II (but not compound I) reduction by ascorbate and tyrosine were slightly diminished in D94V and D94N. The presented biochemical and biophysical data suggest that the Asp[94] to heme linkage is no precondition for the autocatalytic formation of the other two covalent links found in MPO. The findings are discussed with respect to the known active site structure of MPO and its complexes with ligands.

Myeloperoxidase (MPO),[2] eosinophil peroxidase (EPO), lactoperoxidase (LPO), and thyroid peroxidase (TPO) are structurally and functionally related members of a heme peroxidase superfamily (1, 2). With the exception of TPO, they play an important role in the unspecific immune defense system because they catalyze the hydrogen peroxide-mediated oxidation of halide ions and thiocyanate to hypohalous acids and hypothiocyanite, which are effective antimicrobial agents (3–6).

Myeloperoxidase is a cationic dimeric 146-kDa dimer with one monomer containing two polypeptides of 14.5 and 58.5 kDa and a covalently bound modified heme (7–9). The heme is a derivative of protoporphyrin IX in which the methyl groups on pyrrole rings A and C have been modified to allow formation of ester linkages with Glu[242] and Asp[94], respectively. A third covalent link was identified as a sulfonium ion linkage between the sulfur atom of Met[243] and the terminal β-carbon of the vinyl group on pyrrole ring A (Fig. 1) (8, 10). In the homologous peroxidases (EPO, LPO, and TPO) the three-dimensional structure (LPO, Protein Data Bank code 2GJ1) and mass spectrometric analyses show that the heme is also covalently attached to the protein via two ester linkages. It is generally accepted that the cross-linking process occurs autocatalytically and that in LPO the 5-hydroxymethyl bond is formed before the 1-hydroxymethyl bond (11–14). Modes of heme to protein linkages strongly affect the biophysical and biochemical properties of these metalloproteins (15–18).

Recombinant MPO (recMPO) secreted from Chinese hamster ovary cell lines is a single-chain precursor of 84 kDa that failed to undergo proteolytic processing into mature subunits (19). However, its biophysical and biochemical features are identical with the dimeric leukocyte protein (20–22), and it can be produced in sufficient amounts (19) that allow comprehensive spectral and kinetic analysis. Kooter *et al.* (24–26) have already investigated the consequences of exchange of Asp[94], Glu[242], and Met[243] on the spectral features and the overall chlorination and peroxidase activity of the corresponding recMPO variants (23). Exchange of Met[243] caused a significant or even complete loss of its chlorination activity as well as a blue shift of the Soret band of 16–18 nm underlining an important role of the vinyl sulfonium band in reaction with chloride and its unusual spectroscopic properties (21, 26). Exchanges of Asp[94] affected both the overall chlorination and the peroxidase activity and resulted in the formation of two distinct species, one with spectral characteristics of wild-type recMPO and one with spectral features similar to Met[243] variants (25). The loss of the Glu[242] ester bond caused a blue shift of 12 nm in the absorption spectrum and a decrease in the chlorination activity of more than 90% (25).

Here we report the consequences of the disruption of the Asp[94] to ring C linkage in the individual redox reactions of both the halogenation and the peroxidase cycle as well as the role in

* This work was supported by the Austrian Science Fund Project Number P15660. The costs of publication of this article were defrayed in part by the payment of page charges. This article must therefore be hereby marked "*advertisement*" in accordance with 18 U.S.C. Section 1734 solely to indicate this fact.

[1] To whom correspondence should be addressed. Tel.: 43-1-36006-6077; Fax: 43-1-36006-6059; E-mail: christian.obinger@boku.ac.at.

[2] The abbreviations used are: MPO, mature dimeric myeloperoxidase; WT recMPO, wild-type recombinant monomeric myeloperoxidase; LPO, lactoperoxidase; TPO, thyroid peroxidase; 6c, six-coordinated; LS, low spin; HS, high spin; RR, resonance Raman; MCD, monochlorodimedone.

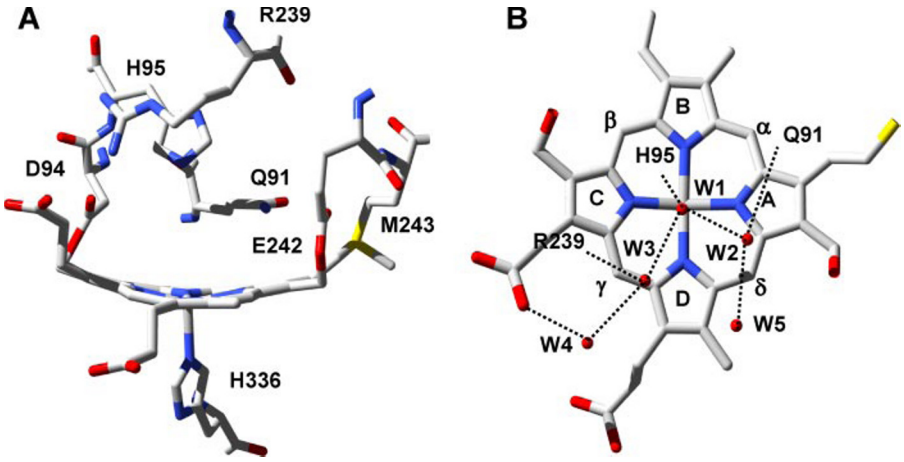

FIGURE 1. *A*, nonplanar porphyrin ring in MPO and its covalent attachments to the protein via two ester bonds (Asp^{94} and Glu^{242}) and one sulfonium ion linkage (Met^{243}). In addition the catalytic residues His^{95}, Arg^{239}, and Gln^{91} are shown, the latter being important in halide binding. *B*, locations of the five water molecules in the distal heme cavity of ferric high spin MPO. The figure was constructed using the coordinates deposited in the Protein Data Bank (accession code 1CXP).

ligand binding and redox chemistry. The simplest reaction of MPO is reversible binding of high spin and low spin ligands to the ferric protein (Reaction 1). Upon reaction with hydroperoxides, MPO undergoes a two-electron oxidation to form compound I (oxoiron(IV) with porphyrin π-cation radical) (27) (Reaction 2). Halides (X^-) reduce compound I directly to native MPO by a two-electron process (Reaction 3) (15–17), thereby forming hypohalous acids (HOX).

$$[Fe(III)(Porph)] + X^- \leftrightarrows [Fe(III)(Porph)]X^-$$
REACTION 1

$$[Fe(III)(Porph)] + ROOH \leftrightarrows [Fe(IV) = O(Porph)^{+\cdot}] + ROH$$
REACTION 2

$$[Fe(IV) = O(Porph)^{+\cdot}] + X^- + H^+ \leftrightarrows [Fe(III)(Porph)] + HOX$$
REACTION 3

Alternatively, compound I is reduced to the ferric enzyme via compound II by two successive one-electron reductions (Reactions 4 and 5) releasing free radicals ($^{\cdot}AH$) (28).

$$[Fe(IV) = O(Porph)^{+\cdot}] + AH_2 \leftrightarrows [Fe(IV) = O(Porph)] + {}^{\cdot}AH$$
REACTION 4

$$[Fe(IV) = O(Porph)] + AH_2 \leftrightarrows [Fe(III)(Porph)] + {}^{\cdot}AH + H_2O$$
REACTION 5

Oxidation of hydrogen peroxide by compound I to give superoxide is unique to myeloperoxidase (Reaction 6) (29–31).

$$[Fe(IV) = O(Porph)^{+\cdot}] + H_2O_2 \leftrightarrows$$

$$[Fe(IV) = O(Porph)] + O_2^{\cdot-} + H^+$$
REACTION 6

Bimolecular rate constants for Reactions 1–6 as well as the effect of exchange of Asp^{94} on the reduction potential of the couple Fe(III)/Fe(II) will be presented and discussed with respect to MPO-typical enzymatic features as well as the proposed autocatalytic mechanism of heme to protein bonds.

EXPERIMENTAL PROCEDURES

Materials—Transfection of recombinant plasmids into Chinese hamster ovary cells, selection and culture procedures for transfected cells, and protein purification protocols were described in detail previously (19). The variants D94N and D94V were produced as described by Kooter *et al.* (21, 25). The concentration of the variants was determined by using an extinction coefficient of 72 mM^{-1} cm^{-1} at 428 nm for D94V and 62 mM^{-1} cm^{-1} at 428 nm for D94N. The latter value takes into account that in D94N the Soret band was split into two maxima (see below) and that the species with the maximum at 413 nm contributed to the absorbance at 428 nm. Principally, extinction coefficients were obtained from the plot of absorbance of the Soret maxima *versus* protein concentration calculated by the method of Bradford (32).

Hydrogen peroxide, obtained as a 30% solution from Sigma, was diluted, and the concentration was determined by absorbance measurement at 240 nm where the extinction coefficient is 39.4 M^{-1} cm^{-1} (33). Hypochlorous acid was obtained from Fluka. The HOCl stock solutions were prepared in 5 mM NaOH and stored in darkness. The HOCl concentration was determined spectrophotometrically ($\epsilon = 350$ M^{-1} cm^{-1} at 292 nm in 5 mM NaOH) shortly before the experiments (34). Peroxide and HOCl stock solutions were prepared fresh twice daily. Cyanide, chloride, tyrosine and ascorbate and all other chemicals were also purchased from Sigma at the highest grade available.

Circular Dichroism Spectrometry—CD spectra were performed on a Jasco J-600 instrument, equipped with a thermostated cell holder, and data were recorded online using a personal computer. Spectra are averages of 12 scans with subtraction of the base line. The quartz cuvette used had a path length of 2 mm. Samples were measured at 25 °C in 5 mM phosphate buffer, pH 7.0, and with protein concentrations of 2 μM.

Overall Halogenation Activity—Halogenation activity was measured spectrophotometrically (Hitachi U-3000) using the monochlorodimedone (MCD) assay. MCD (100 μM) was dissolved in 100 mM phosphate buffer, pH 7.0, and contained either bromide (100 μM) or chloride (100 mM) and 100 nM WT recMPO or Asp^{94} variant. Upon addition of 100 μM H_2O_2 MCD was halogenated. Rates of halogenation were determined from the initial linear part of the time traces using an extinction coefficient for MCD at 290 nm of 19.9 mM^{-1} cm^{-1} (35). One unit is defined as halogenation of 1 μmol of MCD per min and 25 °C.

In addition, the halogenation activity of recMPO and the Asp^{94} variants was measured by continuously monitoring hydrogen peroxide concentration polarographically with a platinum electrode covered with a hydrophilic membrane and fitted to the Amperometric Biosensor Detector 3001 (Universal

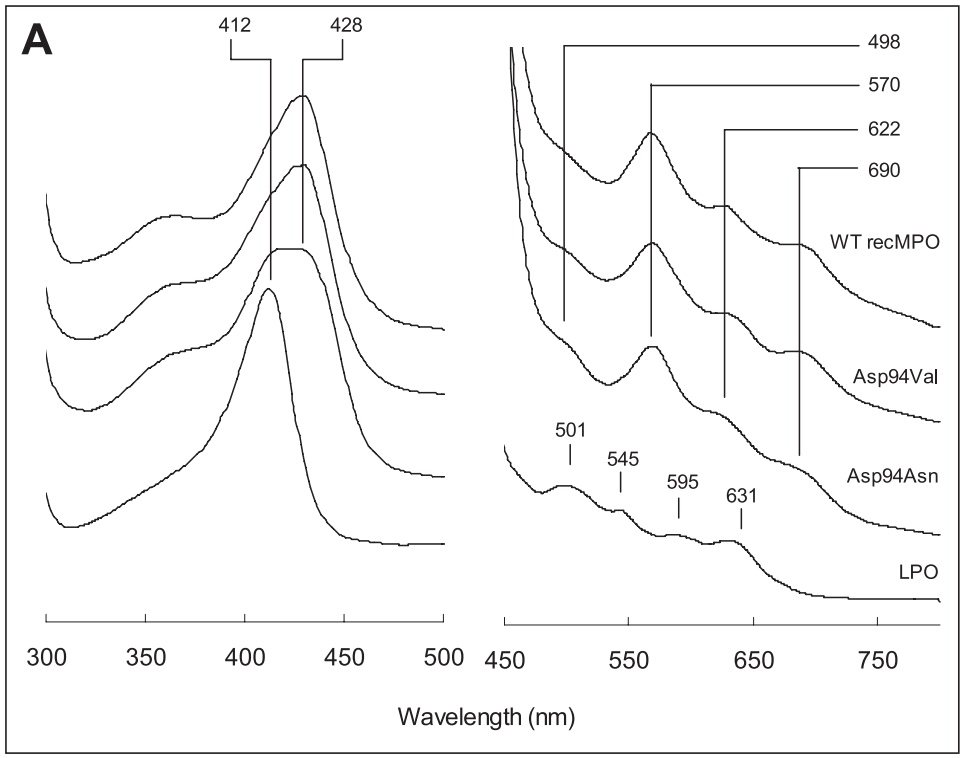

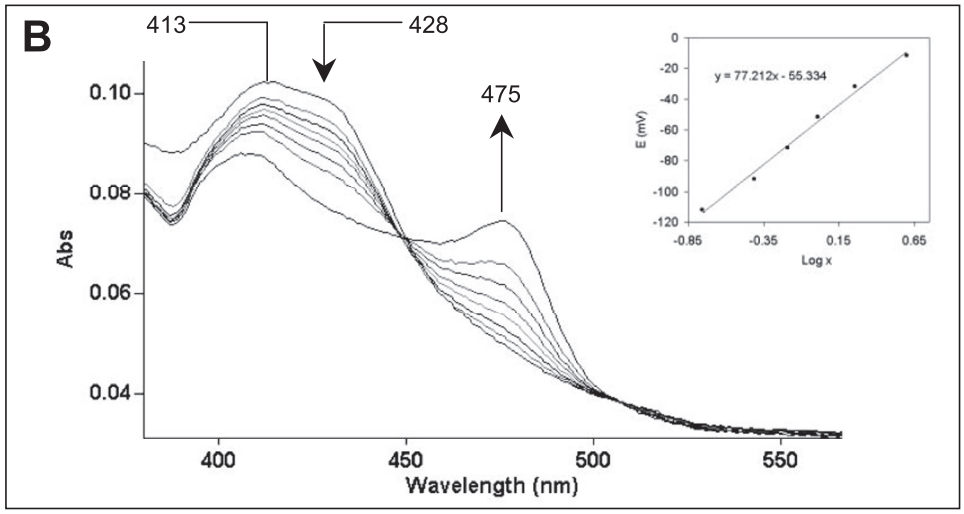

FIGURE 2. *A*, optical absorbance spectra of ferric high spin WT recMPO and the variants D94V and D94N in 100 mM phosphate buffer, pH 7.0. For comparison, the spectrum of bovine LPO is included. *B*, electronic spectra of the MPO variant D94N obtained at various applied potentials. Spectra were recorded at 25 °C. The *inset* depicts the corresponding Nernst plots, where *X* represents $((A^{max}_{\lambda red} - A_{\lambda red})/(A^{max}_{\lambda ox} - A_{\lambda ox}))$ with $\lambda_{ox} = 428$ nm and $\lambda_{red} = 475$ nm.

Sensors, Inc.). The applied electrode potential at pH 7 was 650 mV, and the H_2O_2 electrode filling solution was freshly prepared twice daily. The electrode was calibrated against known concentrations of hydrogen peroxide. All reactions were performed in 100 mM phosphate buffer, pH 7.0, and 25 °C using 100 μM H_2O_2 and various concentrations of halides. Reactions were started by the addition of enzyme (100 nM). One unit is defined as consumption of 1 μmol H_2O_2 per min and 25 °C.

Overall Peroxidase Activity—The one-electron donors ascorbate and tyrosine were used to test the effect of exchange of Asp^{94} on the peroxidase activity (100 mM phosphate buffer, pH 7.0). Ascorbate oxidation (100 μM ascorbate, 100 μM H_2O_2, 100 nM WT recMPO or Asp^{94} variant, 25 °C) was followed by a decrease of absorbance at 290 nm using an extinction coefficient for ascorbate of $\epsilon_{290} = 2.8\ mM^{-1}\ cm^{-1}$ (36). Dityrosine formation from tyrosine (200 μM tyrosine, 100 μM H_2O_2, 50 nM WT recMPO or Asp^{94} variant, 25 °C) was followed spectrofluorimetrically on a Hitachi F-4500 spectrofluorimeter using an excitation wavelength of 325 nm and an emission wavelength at 405 nm (37).

Steady-state Ligand Binding—Equilibrium binding of high spin and low spin ligands to wild-type recMPO or the Asp^{94} variants was performed by spectroscopic titration of 600 nM enzyme in 100 mM phosphate buffer, pH 5.0 or pH 7.0, with increasing concentrations of ligands. Dissociation constants (K_D) of the various enzyme-ligand complexes were determined at 25 °C, according to a previously described method (38). Here, the change in absorbance, $\Delta A_{p\text{-}v}$ (with p and v representing the corresponding absorption maximum (peak) and minimum (valley) in the difference spectrum), was plotted *versus* the ligand concentration. A fitting procedure using $\Delta A_{p\text{-}v} = (\Delta A_{\infty}/[L])/(K_D + [L])$, with [L] being the ligand concentration and ΔA_{∞} the absorbance change at infinite ligand concentration, allowed calculation of K_D.

Transient State Experiments—The stopped-flow apparatus (model SX-18MV) equipped for both conventional and sequential stopped-flow measurements was from Applied Photophysics (UK). For a total of 100 μl/shot into the optical observation cell with 1 cm light path, the fastest time for mixing two solutions and recording the first data point was of the order of 1.3 ms. All measurements were performed at 25 °C.

Cyanide binding and the reaction of D94V or D94N with H_2O_2 and HOCl was measured in the conventional stopped-flow mode by following the decrease of absorbance at the corresponding Soret maxima of the ferric enzyme (428 nm for both variants) or the Soret maxima of the low spin cyanide complexes (456 nm for both variants). In a typical cyanide binding experiment, one syringe contained ~1 μM Asp^{94} variant (100 mM phosphate buffer, pH 7.0), and the second syringe contained at least a 25-fold excess of cyanide (100 mM phosphate

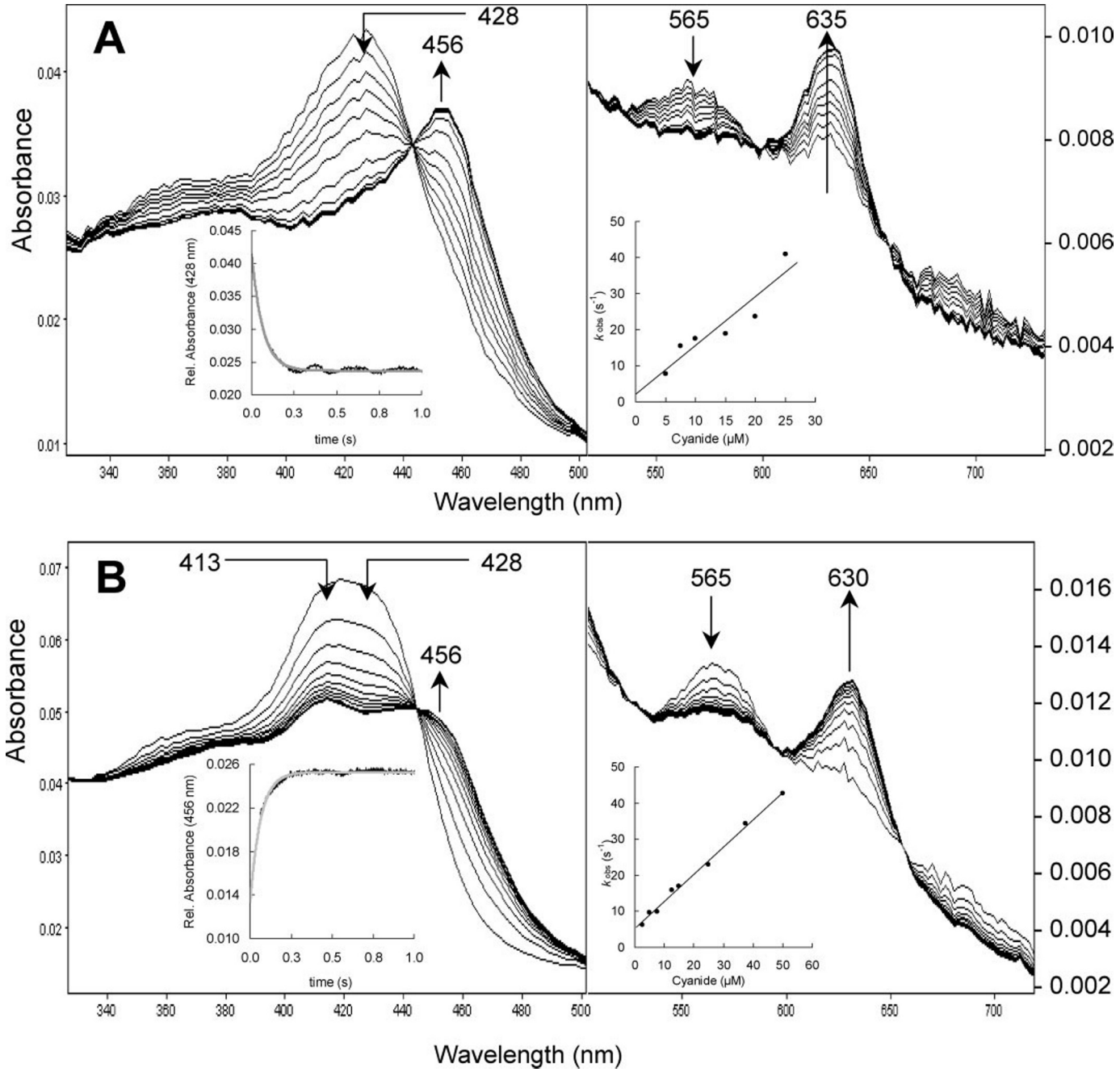

FIGURE 3. **Kinetics and spectral changes of cyanide binding to the myeloperoxidase variants D94V and D94N.** *A,* mixing of 0.7 μM D94V with 10 μM cyanide in 100 mM phosphate buffer, pH 7.0. The *insets* show the time trace at 428 nm of the reaction between 0.35 μM enzyme with 7.5 μM cyanide as well as the plot of determined k_{obs} values *versus* cyanide concentration. *Arrows* indicate spectral changes with time. *B,* mixing of 1.2 μM D94N with 25 μM cyanide in 100 mM phosphate buffer, pH 7.0. The *insets* show the time trace at 456 nm of the reaction between 0.6 μM enzyme with 12 μM cyanide as well as the plot of determined k_{obs} values *versus* cyanide concentration. *Arrows* indicate spectral changes with time.

buffer, pH 7.0). For monitoring compound I formation with H_2O_2 or HOCl, one syringe contained ~1 μM ferric enzyme in 200 mM phosphate buffer, pH 7.0, and the other syringe various concentrations of either H_2O_2 in 5 mM phosphate buffer, pH 7.0, or hypochlorite in 5 mM NaOH. Three determinations were performed for each ligand or oxidant concentration. The mean of the pseudo-first-order rate constants, k_{obs}, was used in the calculation of the second-order rate constants obtained from the slope of a plot of k_{obs} *versus* ligand or oxidant concentration.

Because of the inherent instability of compound I of Asp^{94} variants, the sequential stopped-flow (multimixing) techniques were used for determination of rates of the reaction of compound I with one- and two-electron donors. For wild-type recMPO, the conditions were the same as described for the mature enzyme purified from human blood (22). Typically, the Asp^{94} variant was premixed with a 2-fold excess of H_2O_2 in the aging loop for 500 ms (100 mM phosphate buffer, pH 7.0). Finally, compound I was allowed to react with varying concentrations of electron donors. Halide oxidation was followed by monitoring the absorbance change at 428 nm. Formation of compound II mediated by either ascorbate or tyrosine was followed at 456 nm.

Reactivity of compound II was investigated either by starting with preformed compound II or, alternatively, by following the reaction of compound I with ascorbate or tyrosine to compound II and back to the ferric enzyme (39). In the latter case the resulting biphasic curves showed the initial formation of compound II and then its subsequent reaction with ascorbic acid causing an exponential decrease in absorbance. For example, in the first procedure ~1 μM enzyme was premixed with an equimolar concentration of hydrogen peroxide and a 20-fold excess of homovanillic acid in 100 mM phosphate buffer, pH 7.0. After a delay time of 5 s, compound II was allowed to react with varying concentrations of either ascorbate or tyrosine in the same buffer. Compound II reduction was followed either at the Soret maximum of compound II (456 nm) or ferric enzyme (428 nm).

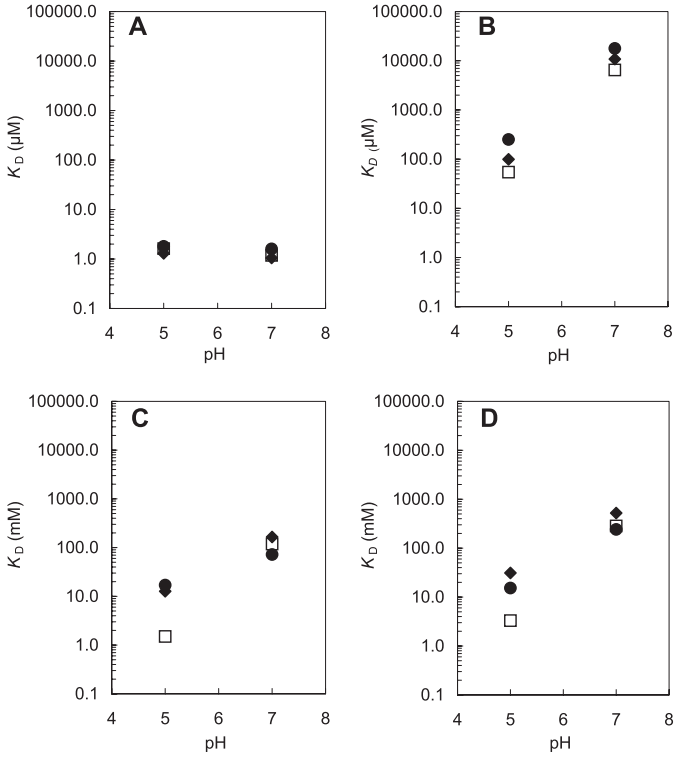

FIGURE 4. **Ligand binding to wild-type recombinant MPO (□), D94V (♦), and D94N (●).** Given are the corresponding K_D values obtained by spectrophotometric titration of ~1 μM enzyme in 100 mM phosphate buffer, pH 7.0 or 5.0, with cyanide (*A*), nitrite (*B*), chloride (*C*), and fluoride (*D*).

TABLE 1

Overall halogenation activity of WT recMPO and the variants D94N and D94A in 100 mM phosphate buffer, pH 7.0, and at 25 °C, containing 100 μM H_2O_2 and 100 nM enzyme

By using the MCD assay (for details see "Experimental Procedures"), 100% specific activities correspond to 0.556 units/mg recMPO (100 mM Cl^-), and 0.610 units/mg MPO (100 μM Br^-), respectively. By using polarographic determination of H_2O_2 consumption, 100% specific activities correspond to 6235 units/mg recMPO (100 mM Cl^-), 1726 units (100 μM Br^-), 8333 units (100 μM SCN^-), and 7706 units (100 μM I^-).

	recMPO	D94N	D94V	Methods
	%	%	%	
Chloride (100 mM)	100	10.0	12.6	MCD assay
	100	9.6	9.5	H_2O_2 electrode
Bromide (100 μM)	100	34.2	29.1	MCD assay
	100	29.1	22.4	H_2O_2 electrode
Thiocyanate (100 μM)	100	97.2	68.1	H_2O_2 electrode
Iodide (100 μM)	100	103.9	54.8	H_2O_2 electrode

All reactions were also investigated using the diode-array detector (Applied Photophysics PD.1) attached to the stopped-flow machine. Normal data sets were analyzed using the Pro-K simulation program from Applied Photophysics, which allowed the synthesis of artificial sets of time-dependent spectra as well as spectral analysis of enzyme intermediates.

Spectroelectrochemistry—All experiments were carried out in an OTTLE cell as described recently for leukocyte MPO (40). The three-electrode configuration consisted of a gold minigrid working electrode (Buckbee-Mears, Chicago), a homemade $Ag/AgCl/KCl_{sat}$ microreference electrode, separated from the working solution by a Vycor set, and a platinum wire as the counter electrode. The reference electrode was calibrated against a saturated calomel electrode before each set of measurements. All potentials are referenced to the standard hydrogen electrode. Potentials were applied across the OTTLE cell with an Amel model 2053 potentiostat/galvanostat. The constant temperature was maintained by a circulating water bath, and the OTTLE cell temperature was monitored with a copper-constant microthermocouple. UV-visible spectra were recorded using a Varian Cary C50 spectrophotometer.

The experiments were carried out under argon in the presence of 20 μM *N*,*N*,*N*′,*N*′-tetramethylphenylenediamine, 2-hydroxy-1,4-naphthoquinone, phenazine methosulfate, and phenazine ethosulfate used as mediators. Samples (1 ml) containing 4.2 μM recMPO and Asp^{94} variants in 0.1 M phosphate buffer and 0.1 M NaCl, pH 7.0, were used. Nernst plots consisted of at least five points and were invariably linear, with a slope consistent with a one-electron reduction.

RESULTS

Electronic Absorption Spectroscopy—The electronic absorption spectra of Fe(III) recMPO and the variants D94V and D94N are shown in Fig. 2. For comparison the spectrum of bovine LPO in its ferric form is included, which has its maxima at 412, 501, 545, 595, and 631 nm. The bandwidth and wavelength of the Soret band as well as the wavelength of the charge transfer bands (CT1) at 631 nm are characteristic of a six-coordinated (6c) high spin (HS) aquo ferric heme (41). The electronic absorption maxima of the ferric form of MPO are red-

TABLE 2

Overall peroxidase activity of WT recMPO and Asp^{94} variants in 100 mM phosphate buffer, pH 7.0, and 25 °C

For details see "Experimental Procedures." One unit is defined as 1 μmol of substrate being oxidized per min. FU indicates arbitrary fluorescence units obtained from fluorimetric monitoring of dityrosine formation.

	WT recMPO	D94N	D94V
Ascorbic acid	3.03 units/mg 100.0%	2.14 units/mg 70.5%	1.98 units/mg 65.2%
Tyrosine	7.7×10^5FU/(min × mg) 100.0%	3.8×10^5 FU/(min × mg) 49.0%	4.1×10^5 FU/(min × mg) 53.2%

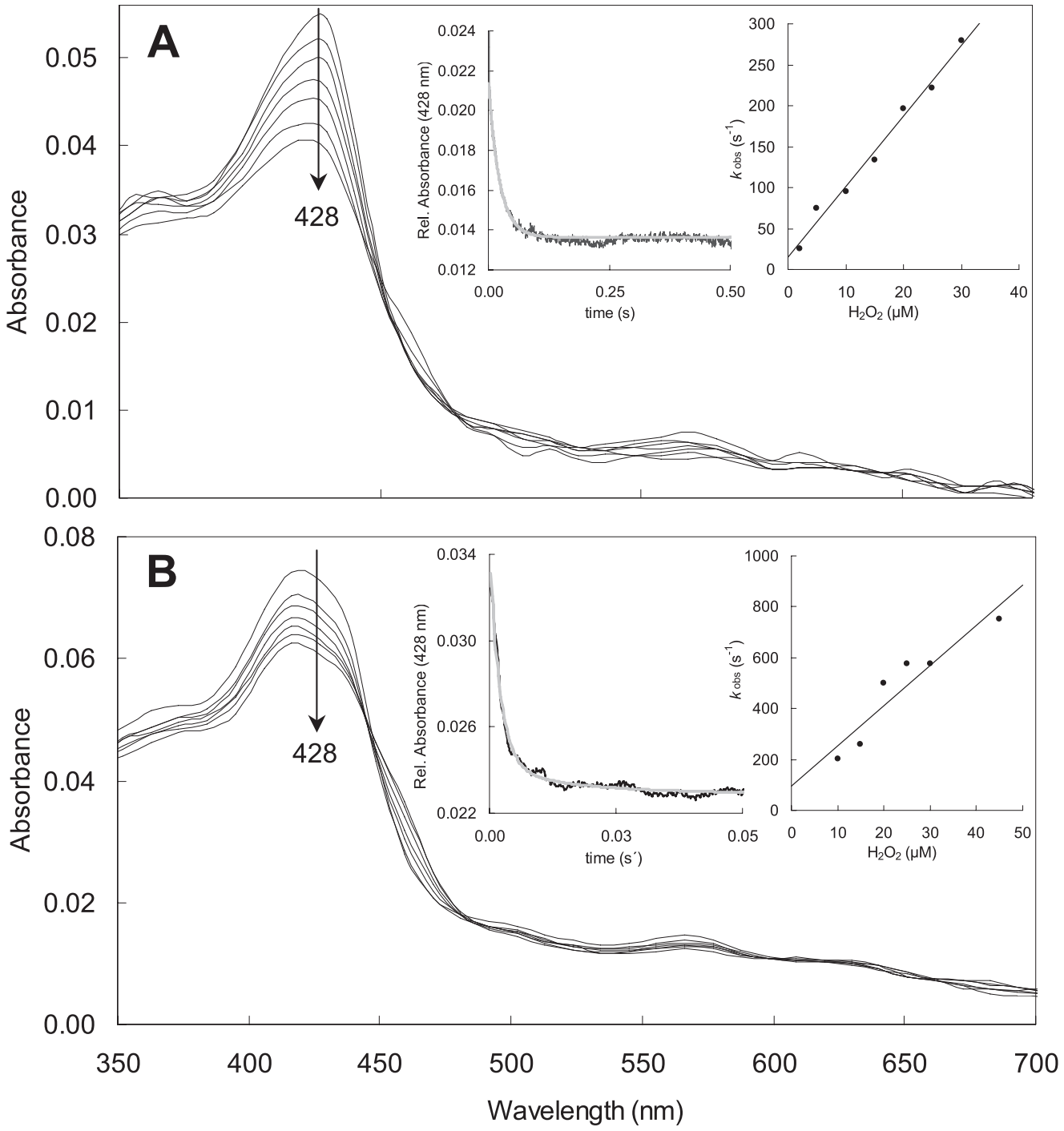

FIGURE 5. **Kinetics of compound I formation of the myeloperoxidase variants D94V and D94N.** *A,* mixing of 0.7 μM D94V with 10 μM hydrogen peroxide in 100 mM phosphate buffer, pH 7.0. The *insets* show the time trace at 428 nm of the reaction between 0.35 μM enzyme with 15 μM H_2O_2 as well as the plot of determined k_{obs} values *versus* H_2O_2 concentration. *Arrow* indicates spectral changes with time. *B,* mixing of 1.2 μM D94N with 20 μM hydrogen peroxide in 100 mM phosphate buffer, pH 7.0. The *insets* show the time trace at 428 nm of the reaction between 0.6 μM enzyme with 20 μM H_2O_2 as well as the plot of determined k_{obs} values *versus* H_2O_2 concentration. *Arrows* indicate spectral changes with time.

shifted compared with LPO. The Soret band of WT recMPO is at 428 nm, and the spectrum shows additional bands at 498, 570, 622, and 690 nm, suggesting that WT recMPO is also 6c HS in the ferric form (42). The spectrum of D94V is similar to WT recMPO with a slight shoulder at the Soret band at 413 nm, whereas in case of D94N the Soret band was split into two maxima, with one maximum at the same wavelength (428 nm) as that of WT recMPO and a blue-shifted maximum (413 nm) similar to that of LPO. The visible spectrum at longer wavelength of both variants suggests a 6c HS state and is very similar to WT recMPO but dissimilar from LPO. It has to be mentioned that, depending on the point in time of protein harvesting from Chinese hamster ovary cells, the signature of the Soret band slightly changed. Generally, in the Soret band of D94V the shoulder at 413 nm became more pronounced in protein expressed by older cells.

TABLE 3

Apparent second-order rate constants for reactions of WT recMPO and Asp^{94} variants in 100 mM phosphate buffer, pH 7.0, and at 25 °C

For comparison data about E242Q (18) are shown. For details see "Experimental Procedures." C-I indicates compound I; C-II indicates compound II; and C-III indicates compound III.

Reaction/substrate	recMPO	E242Q (18)	D94N	D94V
	$\times 10^4\ M^{-1}\ s^{-1}$	$\times 10^4\ M^{-1}\ s^{-1}$	$\times 10^4\ M^{-1}\ s^{-1}$	$\times 10^4 M^{-1}\ s^{-1}$
Native enzyme → C-I				
H_2O_2	1900	78	1600	870
HOCl	2300	75	2400	3000
C-I → native enzyme				
Chloride	3.6	0.0065	0.2	0.15
Bromide	140	5.4	41	15
Thiocyanate	1400	22	1200	490
Iodide	1400	64	1800	590
C-I → C-II				
H_2O_2	3.0	0.14	5.3	0.83
Ascorbate	23	34	24	27
Tyrosine	32	7.4	42	16
C-II → native enzyme				
Ascorbate	1.4	2.1	0.9	1.05
Tyrosine	1.7	0.028	0.5	1.2

The purity numbers (A_{428}/A_{280}) of the investigated proteins were 0.69–0.71 (WT recMPO), 0.54–0.56 (D94V), and 0.43–0.46 (D94N), respectively. Far-UV CD spectra (not shown) demonstrate that the overall structure is predominantly α-helical and that exchange of aspartate 94 by either valine or asparagine did not induce structural changes. If conformational changes did occur, they must have been very localized and minimal and thus were undetected by CD.

Reduction Potential of the Fe(III)/Fe(II) Couple of recMPO and Asp^{94} Variants—Recently, the reduction potential of leukocyte dimeric MPO was shown to be 5 mV at pH 7.0 and 25 °C (40). Here we have measured the electronic spectra of ferric high spin monomeric recMPO at different applied potentials in the OTTLE cell and could determine an E'_0 value of 1 ± 5 mV (not shown), which underlines that the active sites of leukocyte and recMPO exhibit almost identical reactivities (22) and redox properties. Ferrous recMPO and D94V had their Soret band at 475 nm and an additional maximum at 638 nm (not shown). However, upon disruption of the Asp to heme ester bond, the E'_0 value decreased by about 55 mV. Fig. 2*B* shows the electronic spectra of ferric D94N at different applied potentials. It clearly demonstrates that D94N is a mixture of an active and inactive species. Upon reduction only the active species was reduced (direct transition from 428 to 475 nm) (Fig. 2*B*). From the Nernst plot (Fig. 2*B, inset*) the E'_0 was determined to be −55 ± 10 mV.

Binding of Low Spin and High Spin Ligands (Reaction 1)—By binding directly to the heme iron atom cyanide converted the HS ($S = 5/2$) iron state of recMPO to LS ($S = ½$) state, thereby shifting the Soret peak from 428 to 456 nm with a clear isosbestic point at 442 nm. In the visible range a distinct peak at 635 nm evolved with clear isosbestic points at 525, 600, and 657 nm (not shown). In WT recMPO, the monophasic transition of ferric MPO to the MPO-cyanide complex occurred with an apparent bimolecular rate constant of (1.6 ± 0.1) × $10^6\ M^{-1}\ s^{-1}$, pH 7.0. From the intercept of the linear plot (not shown), the dissociation rate constant (k_{off}) was obtained, allowing the calculation of the dissociation constant (K_D) of the recMPO-cyanide complex from the k_{off}/k_{on} ratio (1.9 μM). A very similar value was obtained by spectroscopic titration (1.4 μM). The loss of the ester bond in D94V affected neither the k_{on} rate ((1.3 ± 0.2) × $10^6\ M^{-1}$)) nor the K_D value obtained from either the kinetic plot (2.4 μM) or by spectroscopic titration (1.3 μM). The transition was also monophasic, and the spectral signatures of the cyanide complex fully matched those of WT recMPO (Fig. 3*A*). Investigating the cyanide binding to D94N again revealed that this variant is a mixture of an active and an inactive species. The monophasic transition resulted in a cyanide complex with an absorption spectrum similar to that of D94V (peak maxima at 456 and 630 nm and isosbestic points at 443, 525, 597, and 656 nm). Fig. 3*B* clearly demonstrates that the peak at 413 nm did not shift upon addition of cyanide. This suggests that only the species with its Soret band at 428 nm has an accessible heme cavity and can bind cyanide. For D94N, the calculated k_{on} ((7.5 ± 0.3) × $10^5\ M^{-1}\ s^{-1}$) and the K_D (1.6 μM) values were similar to D94V or WT recMPO. In all three proteins the K_D values at pH 5 were similar to those at pH 7 (Fig. 4*A*).

Similar to cyanide, nitrite binding converts ferric HS to LS MPO (Soret band at 447 nm) (not shown). Nitrite is both a ligand and substrate of MPO (43). Exchange of Asp^{94} only slightly affected nitrite binding at pH 7. The determined K_D values are 6.6 mM (WT recMPO), 10.8 mM (D94V), and 17.8 mM (D94N). Nitrite binding to peroxidases is known to be favored at acidic pH, and this was followed by all three proteins (Fig. 4*B*). The corresponding dissociation constants decreased significantly at pH 5 as follows: 54.4 μM (WT recMPO), 91.1 μM (D94V), and 250 μM (D94N), respectively. As already observed with cyanide binding, in D94N only the species with its Soret maximum at 428 nm could bind nitrite, and the resulting spectral signatures in the visible region were similar to those of the NO_2^- complex with WT recMPO or D94V (not shown).

Halides do not bind directly to the heme. The structure of the MPO-bromide complex has been solved (44) and shows bromide binding at the position of water molecule Wat-2 (Fig. 1*B*). Thus, halides are typical HS ligands, and the spectral changes upon halide binding were relatively small (red-shift of the Soret band 1–3 nm depending on halide; data not shown). Fig. 4, *C* and *D*, depicts the pH dependence of the K_D values obtained by spectrophotometric titration of the corresponding chloride and fluoride complexes. Halide binding was favored at acidic pH. With WT recMPO the K_D values for chloride and fluoride decreased from 118.3 and 284 mM, pH 7.0, to 1.5 and 3.3 mM, pH 5.0, respectively. In contrast to neutral pH, the differences in K_D values between WT and variant proteins increased with decreasing pH (Fig. 4, *C* and *D*). The same tendency was also observed with nitrite and indicates a decreased affinity of anions to the Asp^{94} variants at pH 5. Apparently, the loss of the ester bond hampers to some extent the hydrogen bonding between the anion and the distal site histidine, which in its protonated form has been suggested to stabilize halide or nitrite complexes of MPO (15, 44).

Overall Halogenation and Peroxidase Activity—In the beginning both the chlorinating and brominating activity was measured by monitoring the halogenation of monochlorodimedone at 290 nm and pH 7.0. Compared with WT recMPO (100%), the chlorination activity of both variants was diminished by about 90%, whereas the effect on the bromination activity was smaller

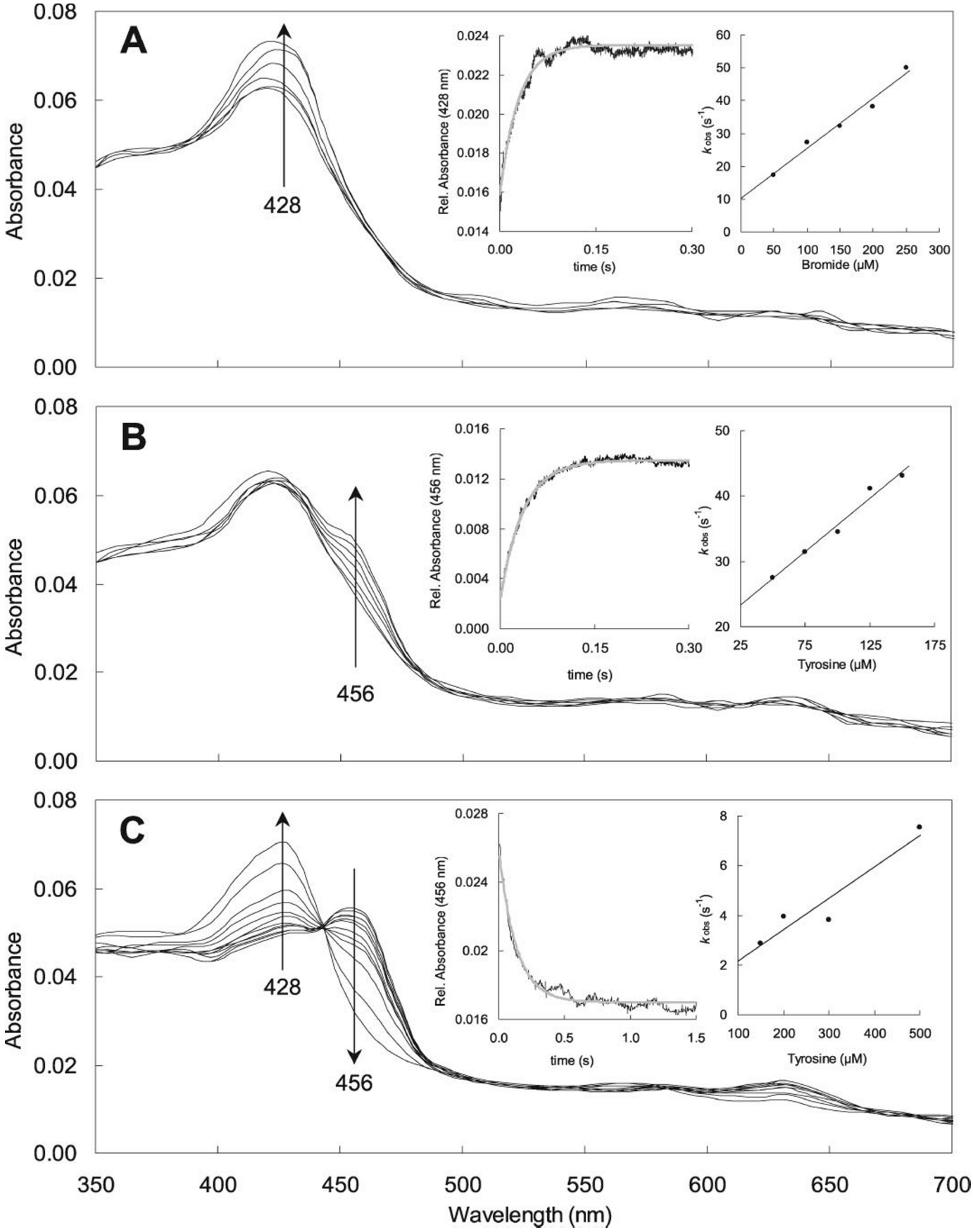
A
Absorbance
428
Rel. Absorbance (428 nm)
time (s)
k_{obs} (s^{-1})
Bromide (μM)
B
Absorbance
456
Rel. Absorbance (456 nm)
time (s)
k_{obs} (s^{-1})
Tyrosine (μM)
C
Absorbance
428
456
Rel. Absorbance (456 nm)
time (s)
k_{obs} (s^{-1})
Tyrosine (μM)
Wavelength (nm)

(about 66–70% loss of activity compared with WT recMPO) (Table 1). Following the consumption of hydrogen peroxide at identical conditions gave similar results (90% loss of H_2O_2 consumption with chloride and 70–77% loss of H_2O_2 consumption with bromide as electron donor). Exchange of Asp^{94} by Asn had no effect on the H_2O_2 consumption rate using thiocyanate and iodide as electron donor. By contrast, the corresponding activities of D94V were diminished by 32 and 45%, respectively (Table 1).

The effect of exchange of aspartate 94 on the peroxidase activity depended on the nature of the electron donor. With both variants ascorbate oxidation was diminished by about 30–35%, whereas the rates of tyrosine oxidation were diminished by about 47–51% (Table 2).

Compound I Formation (Reaction 2)—Compound I of WT recMPO is characterized by a 50% decrease of absorbance in the Soret region. At least a 10-fold excess of H_2O_2 is needed to get the full hypochromicity at 428 nm. The reaction is monophasic, and the apparent bimolecular rate constant is $1.9 \times 10^7\ M^{-1}\ s^{-1}$ at pH 7.0. With both variants compound I formation is also monophasic and needs a slight excess of H_2O_2 (Fig. 5). The calculated rate of compound I formation of D94N is similar, whereas that of D94V was about half the rate of WT recMPO (Table 3). By contrast, the calculated apparent bimolecular rate constants of compound I formation by hypochlorous acid was similar with all three proteins (Table 3). Independent of the oxidant and similar to the results obtained in the ligand binding studies, in the D94N variant only the species with its Soret maximum at 428 nm was redox-active (Fig. 5*B*).

Compound I of myeloperoxidase is not stable. It is well established that in WT recMPO H_2O_2 mediates the compound I to compound II transition thereby releasing superoxide radicals (Reaction 6) (15, 30). By following the reactions presented in Fig. 5 at a longer time scale, the rapidly formed compound I was transformed by H_2O_2 to compound II with its Soret maximum at 456 nm, a clear isosbestic point at 442 nm, and an absorption band at 625 nm (not shown) (9). This counts for both variants and thus confirms that there is only one redox active species in D94N. Although in homologous peroxidases, like EPO or LPO, Reaction 6 is not active (16, 17), both Asp^{94} variants can catalyze the one-electron oxidation of hydrogen peroxide by compound I (Table 3).

Compound I Reduction by Halides (Reaction 3)—Because of the instability of compound I of WT recMPO and both Asp^{94} variants, the sequential stopped-flow mode was used to investigate the role of Asp^{94} in its reduction by two-electron donors. Fig. 6*A* shows the direct reduction of D94V compound I by bromide to the resting state. Typical time traces displayed single-exponential character and the plots of calculated k_{obs} values *versus* bromide concentration were linear (Fig. 6*A*, *insets*). Linear plots were obtained also for chloride, iodide, and thiocyanate (not shown). In general, the impact of exchange of Asp^{94} depended on the nature of the halide. Chloride could still mediate the direct reduction of compound I, but the reaction rate was only 4–5% the rate of WT recMPO (*i.e.* $3.6 \times 10^4\ M^{-1}\ s^{-1}$). The effect was less dramatic with bromide. The variants still exhibited 29% (D94N) and 11% (D94V) of the WT activity, whereas the iodide and thiocyanate oxidation rates of D94N were very similar to that of WT recMPO and diminished by 58–65% in D94V (Table 3).

Compound I and Compound II Reduction by One-electron Donors (Reactions 4 and 5)—Upon addition of ascorbic acid or tyrosine to compound I of both Asp^{94} variants, the sequential formation of compound II and ferric enzyme was observed. Fig. 6, *B* and *C,* depicts the direct transition of D94V compound I to compound II and of preformed compound II back to ferric D94V. Both reactions were mediated by tyrosine. Compound II of both variants exhibited the typical maxima at 456 and 625 nm. Independent of the donor molecule, the resulting time traces displayed single-exponential character, and the apparent second-order rate constants were determined from the corresponding linear plots (Fig. 6, *B* and *C, insets*). Very similar rates of compound II reduction were obtained when compound II formation and reduction were followed in one reaction, and the k_{obs} values were obtained from the latter part of the resulting biphasic curve monitored at 456 nm (Table 3). As already observed in steady-state kinetic experiments, Asp^{94} does not play an important role in the peroxidase activity. With both hydrophilic ascorbate and aromatic tyrosine, the calculated apparent bimolecular rate constants of compound I and compound II reduction were similar or slightly diminished compared with those of WT recMPO.

DISCUSSION

Here we have investigated the role of Asp^{94} to heme linkage in redox chemistry and catalysis of myeloperoxidase. Based on the presented data and the recently published work on E242Q (18), it is now possible to discuss the role of these ester linkages in ligand and substrate binding as well as in the interconversion of the redox intermediates that participate in both the halogenation and the peroxidase cycle.

Aspartate 94 plays a prominent role in MPO structure. It has to be emphasized that it is neighbored to the distal His^{95} (Fig. 1*A*) and to Asp^{96}. The latter functions as a ligand of a calcium ion. All these residues are part of the small polypeptide of MPO and are highly conserved in mammalian peroxidases (9). Asp^{96} is important for the interaction between the small and large polypeptide chain of MPO because all other ligands that bind Ca^{2+} in a pentagonal bipyramidal geometry are provided by the large polypeptide (9). From the presented data we conclude that the loss of the Asp^{94} ester bond had no obvious effect on the overall protein structure and the distal site architecture around

FIGURE 6. **Interconversion of compound I and compound II of the myeloperoxidase variant D94V.** *A,* reaction of 1.2 μM D94V compound I with 200 μM bromide followed in 100 mM phosphate buffer, pH 7.0, and 25 °C. For details in compound I formation in the sequential stopped-flow mode see "Experimental Procedures." The *insets* show a typical time trace followed at 428 nm as well as a plot of calculated k_{obs} values *versus* bromide concentration. *B,* reaction of 1.2 μM D94V compound I with 100 μM tyrosine. The *inset* depicts the time trace of the reaction between 0.6 μM D94V compound I with 50 μM tyrosine followed at 456 nm in 100 mM phosphate buffer, pH 7.0, and 25 °C, as well as the plot of calculated k_{obs} values *versus* tyrosine concentration. *C,* reaction of 1.2 μM preformed compound II (see "Experimental Procedures") with 100 μM tyrosine. The *insets* show a typical time trace of the reaction of 0.6 μM D94V with 500 μM tyrosine followed at 456 nm in 100 mM phosphate buffer, pH 7.0, and 25 °C, as well as the plot of calculated k_{obs} values *versus* tyrosine concentration.

His^{95} (Fig. 1). This conclusion is based on the following: (i) the identical overall secondary structure obtained by CD spectroscopy; (ii) the spectral features observed in UV-visible and resonance Raman spectroscopy (42) that indicate the presence of 6c HS proteins in the resting state as in WT recMPO; and (iii) the similar reactivity of both variants and WT recMPO with cyanide and hydrogen peroxide, which needs His^{95} to be in a proper position to function as proton acceptor and donor.

The conclusion drawn above does not fully apply to D94N, which contains two species that could not be separated by various chromatographic methods (not shown). D94N exhibited two Soret bands, one at 428 nm corresponding to WT recMPO, and the position of the other is around 413 nm and at first sight similar to LPO or the M243Q variant described by Kooter *et al.* (24). The UV-visible spectral features suggest that the latter species, besides the loss of the ester bond involving Asp^{94}, had also lost the sulfonium linkage. However, a recently performed RR study on D94N in comparison with M243T showed that there is no clear evidence in D94N of a species with RR spectral features similar to M243T (42). In addition, the data presented in this work clearly showed that the Soret band at 413 nm could not be affected by low spin ligands nor did it participate in redox transitions. This is in contrast to M243Q (24). Thus it is reasonable to assume that the D94N species with its Soret band at 413 nm is a misfolded active site that impairs access of ligands and substrates, whereas the species with its Soret band at 428 nm was fully active and similar to D94V.

In both Asp^{94} variants the presence of the sulfonium ion linkage is evidenced by their WT-like UV-visible and RR spectra (42) as well as their capacity to oxidize chloride. Similarly, based on RR and EPR studies (25) as well as on its sensitivity to autocleavage of the Met^{243}–Pro^{244} peptide bond (10, 24, 25), it was proposed that E242Q has an intact Met^{243} to heme linkage. Nevertheless, the impact of loss of the two individual ester bonds on ligand binding and redox reactivity is significantly different. In E242Q both cyanide binding as well as compound I formation by either hydrogen peroxide or hypochlorous acid were decelerated, whereas the impact of loss of the ester bond involving Asp^{94} on these reactions was negligible. Generally, the cyanide complex of a heme peroxidase is a useful analogue of the unstable redox intermediate compound I. The crystal structure of the low spin cyanide-MPO complex (44) demonstrates that cyanide binding causes displacement of the water molecule Wat-1 (Fig. 1*B*), which is positioned approximately midway between N$^{\epsilon}$ of His^{95} and the heme iron in ferric MPO. The cyanide nitrogen is hydrogen-bonded with the distal histidine. As already mentioned above, the high similarities between WT recMPO and the Asp^{94} variants in binding of LS ligands (k_{on} and K_D values) suggest that both the access to and the geometry of the distal heme cavity were not altered substantially upon exchange of Asp^{94}. The same conclusion can be drawn from the stopped-flow measurements of compound I formation. In compound I formation by hydrogen peroxide a transient Fe(III)-OOH intermediate is formed, followed by fast heterolytic cleavage of the O–O bond, leading to formation of compound I and expulsion of a water molecule (Reaction 2). In both reaction steps the distal histidine is essential and must be in a proper position and orientation. WT-like rates of compound I formation in both Asp^{94} variants with H_2O_2 and HOCl thus underline the conclusion drawn above.

The effect of disruption of the two ester linkages on halide oxidation is also different. Exchange of Asp^{94} had no effect on iodide and thiocyanate oxidation, whereas bromide and chloride oxidation by D94N and D94V compound I were 3–9- and 18–24-fold slower compared with WT recMPO. By contrast, in E242Q the chloride, bromide, iodide, and thiocyanate oxidation rates were 550, 25, 21, and 63 times decreased (18). This reflects the neighborhood of Glu^{242} to the halide-binding site in MPO. It has been shown by Fiedler *et al.* (8) that in the MPO-bromide complex the halide replaces the water molecule Wat-2 (Fig. 1*B*), which is hydrogen-bonded to the side chain of a conserved Gln^{91}. Additional interactions of the bound bromide occur between water molecules Wat-1 and Wat-5, and the closest heme atom to the bromide is the methylene bridge carbon δ between pyrrole rings A and D (Fig. 1*B*). Some differences were found in the structure of the MPO-cyanide-bromide complex, which could serve as a model of bromide bound to compound I. Here bromide binds at the position of water molecule Wat-5, and the closest protein atoms were found to be the C$^{\gamma}$ atom of Glu^{242} and the C$^{\gamma}$ of Arg^{239}, and the nearest neighboring heme atom is the pyrrole ring D methyl carbon. From these structural data, it is clear that disruption of the Glu^{242} ester bond to pyrrole ring A affects electron donation from all halides because Glu^{242}, together with Met^{243}, seems to optimize the halide positioning and electron transfer to the δ-meso carbon of the porphyrin π-cation radical of compound I. Asp^{94} is not directly involved in halide binding. Nevertheless its capacity in chloride and bromide oxidation is lower than in WT recMPO. Because the amino acid geometry at the distal heme side is apparently almost unchanged in D94V and the active species in D94N, it is tempting to speculate that the more flexible heme in the variants exhibits a lower reduction potential (E'_0) of the redox couple compound I/ferric peroxidase, which has been shown to be 1.16 V at pH 7.0 and 25 °C in MPO purified from human leukocytes (45). This is supported by the presented spectroelectrochemical data. Upon exchange of Asp^{94} E'_0 [Fe(III)/Fe(II)] was reduced by about 55 mV. This, together with resonance Raman spectroscopy data, which demonstrated lowering of the out-of-plane distortion of pyrrole ring C in D94V (42), clearly demonstrates a correlation between heme distortion and redox properties.

Both variants are still more active in bromide oxidation than lactoperoxidase (17), which has a corresponding reduction potential of 1.09 V (46), whereas the chlorination activity is comparable with that of eosinophil peroxidase (16), which has an E'_0 value of 1.1 V (45, 47). In addition to an unfavorable modification of the redox properties, the binding and oxidation of small substrates like chloride seem to be very sensitive to subtle changes of the hydrogen bonding network. In MPO, water molecules fill a funnel-shaped channel forming an extended network of hydrogen bonds that leads from the distal cavity to the surface of the protein (8). Redox thermodynamic investigations (40) have demonstrated only small reduction-induced solvent reorganization effects in MPO purified from human leukocytes compared with plant-type peroxidases, which could be functionally relevant. The low mobility of water

molecules in the distal heme cavity seems to be crucial in fixing the position of chloride. The presence of all three heme to ester linkages exclusively in MPO will constrict the mobility of the solvent. Thus, loss of the Asp^{94} ester bond most likely decreases the reduction potential of the couple compound I/ferric peroxidase and increases the mobility of the solvent thereby destabilizing the binding of small high spin ligands. The observed increased K_D values of chloride and fluoride at acidic pH underline this hypothesis.

The presented data also underline that the Asp^{94} to heme ester bond does not participate in the binding and oxidation of one-electron donors. Aromatic donors are known to bind at the hydrophobic region at the entrance to the distal heme cavity above the pyrrole ring D (48). The pyrrole ring A neither contributes to the optimum positioning of one-electron donor nor to electron transfer to the heme.

The present paper also suggests that the formation of the second ester bond and the sulfonium ion linkage can occur in the absence of Asp^{94}. It is well established that the heme to protein bonds in mammalian peroxidases are formed through a self-processing mechanism (49). From studies on bovine LPO and the Asp^{225} and Glu^{375} variants (corresponding to Asp^{94} and Glu^{242} in MPO), it was concluded that the 5-hydroxymethyl bond (Asp^{225}) may form before the 1-hydroxymethyl bond (12). The presented spectral and kinetic data clearly demonstrate that this pattern is not followed by MPO. Especially the spectral features, the still very positive reduction potential of −55 mV (compared with −190 mV of LPO), and the remaining capacity to oxidize chloride suggest that both covalent links at pyrrole ring A are intact in the Asp^{94} variants. Studies on plant-type peroxidase variants have revealed that there are no specific requirements for autocatalytic ester bond formation other than the presence of an appropriately located carboxyl side chain (50). Apparently in both MPO Asp^{94} variants Glu^{242} and Met^{243} are located properly to allow autocatalytic bond formation.

Summing up, disruption of the Asp^{94} ester bond in myeloperoxidase has no effect on the kinetics and thermodynamics of the formation of low spin complexes. The two-electron oxidation of the 6c HS ferric proteins by H_2O_2 or HOCl is similar to wild-type recMPO as is the two-electron reduction of compound I by iodide and thiocyanate. The increase in heme flexibility lowered the reduction potential of Fe(III)/Fe(II) and most probably of higher oxidation states thereby decelerating the rate of compound I reduction by chloride and bromide. An intact Asp^{94} to heme linkage is no precondition for the autocatalytic formation of the other two covalent links found in myeloperoxidase.

REFERENCES

1. Taurog, A. (1999) *Biochimie* (*Paris*) **81,** 557–562
2. Daivasu, H., and Toh, H. (2000) *J. Mol. Evol.* **31,** 433–445
3. Klebanoff, S. J. (1970) *Science* **169,** 1095–1097
4. Harrison, J. E., and Schultz, J. (1976) *J. Biol. Chem.* **251,** 1371–1374
5. Wang, J., and Slungaard, A. (2006) *Arch. Biochem. Biophys.* **445,** 256–260
6. Ihalin, R., Loimaranta, V., and Tenovuo, J. (2006) *Arch. Biochem. Biophys.* **445,** 261–268
7. Zeng, J., and Fenna, R. E. (1992) *J. Mol. Biol.* **226,** 185–207
8. Fiedler, T. J., Davey, R. E., and Fenna, R. E. (2000) *J. Biol. Chem.* **275,** 11964–11971
9. Furtmüller, P. G., Zederbauer, M., Jantschko, W., Helm, J., Bogner, M., Jakopitsch, C., and Obinger, C. (2006) *Arch. Biochem. Biophys.* **445,** 199–213
10. Taylor, K. L., Strobel, F., Yue, K. T., Ram, P., Pohl, J., Woods, A. S., and Kinkade, J. M. (1995) *Arch. Biochem. Biophys.* **316,** 635–642
11. Suriano, G., Watanabe, S., Ghibaudi, E. M., Bollen, A., Ferrari, R. P., and Moguilevsky, N. (2001) *Bioorg. Med. Chem. Lett.* **11,** 2827–2831
12. Colas, C., Kuo, J. M., and Ortiz de Montellano, P. R. (2002) *J. Biol. Chem.* **277,** 7191–7200
13. Oxvig, C., Thomsen, A. R., Overgaard, M. T., Sorensen, E. S., Hojrup, P., Bjerrum, M. J., Gleigh, G. J., and Sottrup-Jensen, L. (1999) *J. Biol. Chem.* **274,** 16953–16958
14. Fayadat, L., Niccoli-Sire, P., Lanet, J., and Franc, J.-L. (1999) *J. Biol. Chem.* **274,** 10533–10538
15. Furtmüller, P. G., Burner, U., and Obinger C. (1998) *Biochemistry* **37,** 17923–17930
16. Furtmüller, P. G., Burner, U., Regelsberger, G., and Obinger, C. (2000) *Biochemistry* **39,** 15578–15584
17. Furtmüller, P. G., Jantschko, W., Regelsberger, G., Jakopitsch, C., Arnhold, J., and Obinger, C. (2002) *Biochemistry* **41,** 11895–11900
18. Zederbauer, M., Jantschko, W., Neugschwandtner, K., Jakopitsch, C., Moguilevsky, N., Obinger, C., and Furtmüller, P. G. (2005) *Biochemistry* **44,** 6482–6491
19. Moguilevsky, N., Garcia-Quintana, L., Jacquet, A., Tournay, C., Fabry, L., Pierard, L., and Bollen, A. (1991) *Eur. J. Biochem.* **197,** 605–614
20. Jacquet, A., Deby, C., Mathy, M., Moguilevsky, N., Deby-Dupont, G., Thirion, A., Goormaghtigh, E., Garcia-Quintana, L., Mollen, A., and Pincemail, J. (1991) *Arch. Biochem. Biophys.* **291,** 132–138
21. Kooter, I. M., Pierik, A., Merkx, M., Averill, B. A., Moguilevsky, N., Bollen, A., and Wever, R. (1997) *J. Am. Chem. Soc.* **119,** 11542–11543
22. Furtmüller, P. G., Jantschko, W., Regelsberger, G., Jakopitsch, C., Moguilevsky, N., and Obinger, C. (2001) *FEBS Lett.* **503,** 147–150
23. Jacquet, A., Garcia-Quintana, L., Delleersnyder, V., Fenna, R., Bollen, A., and Moguilevsky, N. (1994) *Biochem. Biophys. Res. Commun.* **202,** 73–81
24. Kooter, I. M., Moguilevsky, N., Bollen, A., Sijtsema, N. M., Otto, C., and Wever, R. (1997) *J. Biol. Inorg. Chem.* **2,** 191–197
25. Kooter, I. M., Moguilevsky, N., Bollen, A., Sijtsema, N. M., Otto, C., Dekker, H. L., and Wever, R. (1999) *Eur. J. Biochem.* **264,** 211–217
26. Kooter, I. M., Moguilevsky, N., Bollen, A., van der Veen, L. A., Otto, C., Dekker, H. L., and Wever, R. (1999) *J. Biol. Chem.* **274,** 26794–26802
27. Dolphin, D., Forman, A., Borg, D. C., Fajer, J., and Felton, R. (1971) *Proc. Natl. Acad. Sci. U. S. A.* **68,** 614–618
28. Dunford, H. B. (1999) *Heme Peroxidases,* pp. 349–385, Wiley-VCH, New York
29. Hoogland, H., Dekker, H. L., van Riel, C., Kuilenburg, A., Muijsers, A. O., and Wever, R. (1988) *Biochim. Biophys. Acta* **955,** 337–345
30. Marquez, L. A., Huang, J. T., and Dunford, H. B. (1994) *Biochemistry* **33,** 1447–1454
31. Furtmüller, P. G., Burner, U., Jantschko, W., Regelsberger, G., and Obinger, C. (2000) *FEBS Lett.* **484,** 139–143
32. Bradford, M. (1976) *Anal. Biochem.* **72,** 248–254
33. Nelson, D. P., and Kiesow, L. A. (1972) *Anal. Biochem.* **49,** 474–478
34. Morris, C. (1966) *J. Phys. Chem.* **70,** 3798–3805
35. Kettle, A. J., and Winterbourn, C. C. (1988) *Biochim. Biophys. Acta* **957,** 185–191
36. Nakano, Y., and Asada, K. (1981) *Plant Cell Physiol.* **22,** 867–880
37. Marquez, L. A., and Dunford, H. B. (1995) *J. Biol. Chem.* **270,** 30434–30440
38. Ferrari, R. P., Ghibaudi, E. M., Traversa, S., Laurenti, E., De Gioia, L., and Salmona, M. (1997) *J. Inorg. Biochem.* **68,** 17–26
39. Jantschko, W., Furtmüller, P. G., Allegra, M., Liveira, M. A., Jakopitsch, C., Regelsberger, G., and Obinger, C. (2002) *Arch. Biochem. Biophys.* **398,** 12–22
40. Battistuzzi, G., Bellei, M., Zederbauer, M., Furtmüller, P. G., Sola, M., and Obinger, C. (2006) *Biochemistry* **45,** 12750–12755
41. Smulevich, G., Neri, F., Willemsen, O., Choudhury, K., Merzocchi, M. P., and Poulos, T. (1995) *Biochemistry* **34,** 13485–13490
42. Brogioni, S., Feis, A., Marzocchi, M. P., Zederbauer, M., Furtmüller, P. G., Obinger, C., and Smulevich, G. (2006) *J. Raman Spectrosc.* **37,** 263–276
43. Burner, U., Furtmüller, P. G., Kettle, A. J., Koppenol, W. H., and Obinger,

C. (2000) *J. Biol. Chem.* **275,** 20597–20601
44. Blair-Johnson, M., Fiedler, T., and Fenna, R. (2001) *Biochemistry* **40,** 13990–13997
45. Arnhold, J., Furtmüller, P. G., Regelsberger, G., and Obinger, C. (2001) *Eur. J. Biochem.* **268,** 5142–5168
46. Furtmüller, P. G., Arnhold, J., Jantschko, W., Zederbauer, M., Jakopitsch, M., and Obinger, C. (2005) *J. Inorg. Biochem.* **99,** 1220–1229
47. Arnhold, J., Furtmüller, P. G., and Obinger, C. (2003) *Redox Rep.* **8,** 179–186
48. Davey, C. A., and Fenna, R. E. (1996) *Biochemistry* **35,** 10967–10973
49. Colas, C., and Ortiz de Montellano, P. R. (2003) *Chem. Rev.* **103,** 2305–2332
50. Colas, C., and Ortiz de Montellano, P. R. (2004) *J. Biol. Chem.* **279,** 24131–24140